

UNIVERSITY of CALIFORNIA
SANTA CRUZ

**THERMAL EVOLUTION OF URANUS AND NEPTUNE WITH
CONDENSATION-INHIBITED CONVECTION**

A thesis submitted in partial satisfaction of the
requirements for the degree of

BACHELOR OF SCIENCE

in

ASTROPHYSICS

by

Robert Schroder

November 2020

Copyright © by

Robert Schroder

2020

Abstract

Thermal Evolution of Uranus and Neptune with Condensation-inhibited Convection

by

Robert Schroder

This will be the last section written, once we have finished our results and conclusion.

Contents

List of Figures	v
List of Tables	vi
Dedication	vii
Acknowledgements	viii
1 Introduction	1
2 Model	3
2.1 Historical Work	3
2.2 Three-layer Model with Dry Adiabat	4
2.3 Inclusion of Moist Adiabat Within Outer Envelope	6
2.4 Temperature Jump Across the Water Condensation Zone	8
2.5 Thermal Evolution of Model	9
3 Results	11
3.1 Condensation-inhibited Convection	11
3.2 Formation of Radiative Zone	11
3.3 Thermal Evolution of Uranus and Neptune	11
4 Discussion and Conclusions	15
A Some Ancillary Stuff	16

List of Figures

2.1	A Standard Interior Structure Model	5
2.2	Interior Structure for Moist Adiabat	7
3.1	Inhibition of convection on Uranus	12
3.2	Inhibition of convection on Uranus	13
3.3	2 Figures side by side	14

List of Tables

To Who,

M ention to who, if anyone, here

Acknowledgements

I'd like to thank....

1

Introduction

Giant planets radiate away their latent heat of formation through the top of their atmosphere. If they cool to a point where the amount they radiate away is equal to the amount of radiation they receive from their parent star, they enter thermal equilibrium with their surroundings. At the present time, the giant planets in our solar system: Saturn, Jupiter, and Neptune, all have effective temperatures greater than their equilibrium temperature, an intrinsic heat source, except for Uranus. Observations of Uranus show a planet that appears to be in thermal equilibrium with its parent star, a planet with no intrinsic temperature, cooler than its more distant neighbor, Neptune, a planet of similar mass and composition. Thermal evolution models for Uranus have not matched observation, instead predicting a warmer effective temperature at 4.6 Gyr, the current age of the solar system.(Fortney et al., 2011), (M. Podolak, 1991), (W.B. Hubbard, 1995), (L. Scheibe, 2019) [There are other papers by Nettelmann 2013, Linder 2019 that I haven't looked at yet].

There have been various attempts to explain Uranus' cool temperature. Early

investigations posited that a stratified interior, possibly stable against convection, would allow heat to be trapped deep within the the interior.(M. Podolak, 1991). Later work built on this idea, investigating the formation of stable condensation zones(Friedson & Gonzales, 2017), (Leconte et al., 2017), and (Guillot, 1995), and thermal boundary laters(N. Nettelmann, 2016), that would inhibit convection . It was speculated that the presence of these condensation zones could trap heat deep within the interior, allowing the envelope above to cool more rapidly, thereby lowering the planet's effective temperature.

In this paper, we investigate whether stable water condensation zones form within in the interiror of Uranus and Neptune, and present their potential impact on the thermal evolution of the these planets. ... We use the model described in chapter 2.1 as our baseline... The specifics of our model is described in chapter 2.2.

2

Model

2.1 Historical Work

The physics of the interior structure of the solar system gas and ice giants, and attempts to model their thermal evolution, date back to the mid to late twentieth century, after the first observation of Jupiter's intrinsic temperature by Low (1966), with subsequent investigations into the theory of giant planet structure and evolution(Hubbard, 1977b), (Hubbard, 1977a), (M. Podolak, 1991). We begin with a description of the physics of our baseline structure model, starting with the conservation of mass:

$$\frac{dm}{dr} = 4\pi r^2 \rho \quad (2.1)$$

where dm is the mass contained within a sphere of radius r , and $\rho(r)$ is the density at radius r . Hydrostatic equilibrium is also assumed and described by:

$$\frac{dP}{dr} = -\frac{Gm\rho}{r^2} \quad (2.2)$$

where P is the pressure and G is the gravitational constant.

2.2 Three-layer Model with Dry Adiabat

We employ a three-layer interior structure, seen schematically in Figure 2.1. At the center of the planet is a core made of rock and ice. Moving outward, the inner envelope is H_2O dominated, with uniform concentrations of H , He , and H_2O . We use the MAZEVET equation of state (EOS) (S. Mazevet & Potekhin, 2019) to define the structure of the inner envelope. The outer envelope, below 10 bars, contains trace amounts of H_2O , but is mostly H and He , dominated, and utilizes the MH13SCVH EOS (Y. Miguel & Fayon, 2018).

Historically, interior structure models have assumed that the interiors are composed of compressible gasses that are statically unstable and fully convective. In a dry-convective model such as this, a parcel of gas rises as its temperature increases while its pressure remains constant. This process happens without the addition or loss of heat from the parcel, a process referred to as adiabatic. Furthermore, while there may be a critical concentration for a condensable species, all this dry model does not allow for condensation. The temperature-pressure profile follows a dry adiabat gradient(R. Kippenhahn, 2012), given by :

$$\nabla_{\text{ad}} = \left(\frac{\partial \ln T}{\partial \ln P} \right)_s \quad (2.3)$$

Finally, beyond the outer envelope is the atmosphere. When modeling the thermal evolution of gas and ice giants, it has long been recognized that model atmospheres constitute an outer boundary condition for interior structure models, providing key inputs that impact cooling times for interior structure models. Our work considers both (Harold

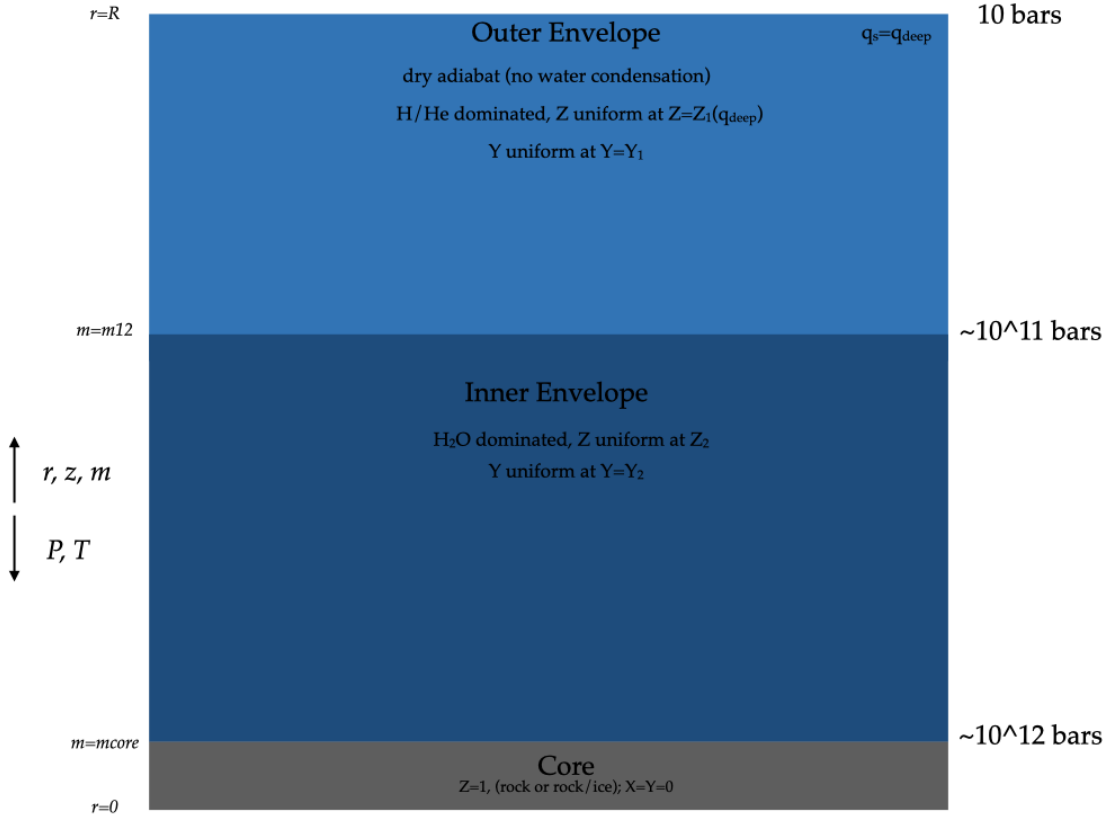


Figure 2.1: The structure for a fully convective, dry adiabatic interior. In this model, the inner and outer envelopes are assumed to be well mixed, fully convective, and following a dry adiabat. The core is composed of rock and ice. The inner envelope is water dominated, with uniform concentrations of hydrogen, helium, and water; whereas, the outer envelope is hydrogen and helium dominated, with trace amounts of water. The 'atmosphere' exists above 10 bars.

C. Graboske & Olness, 1975) and (Fortney et al., 2011) model atmospheres. Unless otherwise stated, our results will utilize the Fortney 2011 model atmospheres.

2.3 Inclusion of Moist Adiabat Within Outer Envelope

Our interior structure model departs from the standard model described above by adding a moist adiabatic layer to the outer envelope that, under favorable conditions, allows for the condensation of H_2O . Gases condense at sufficiently low temperatures or high pressures(cite pierrehumbert). Condensation of a gas is characterized by its saturation vapor pressure, P_{sat} , given by:

$$P_{\text{sat}}(T) = P_{\text{sat}}(T_0)e^{-\frac{1}{R_{\text{gas}}} \left(\frac{1}{T} - \frac{1}{T_0} \right)} \quad (2.4)$$

where R_{gas} is the gas constant for the condensable species. When the partial pressure of a gas, P_{gas} , is less than P_{sat} , the parcel of gas is 'unsaturated'. When $P_{\text{gas}} = P_{\text{sat}}$, the gas is 'saturated'. And, when $P_{\text{gas}} > P_{\text{sat}}$, the parcel is 'supersaturated'. Each condensable species has its own saturation vapor pressure.

The condensation of water in the interior of hydrogen-dominated atmospheres has some notable differences with our experience of water condensation within our own planet's atmosphere (Leconte et al., 2017) (Friedson & Gonzales, 2017) (Guillot, 2019) (Guillot, 1995). On Earth, H_2O lighter than the background air, which is composed primarily of N_2 . So, while condensation of water in the interior of ice giants does release heat through the latent heat of condensation, which in the presence of a heavier background gas would result in an instability, the situation is different when the background is hydrogen-helium dominated. In this case, a strong vertical gradient in mean molecular weight arises, creating a negative buoyancy. This may result in the formation of a layer that is stable against convection (citations).

If condensation zone forms, it may be stable against convection. Convection is

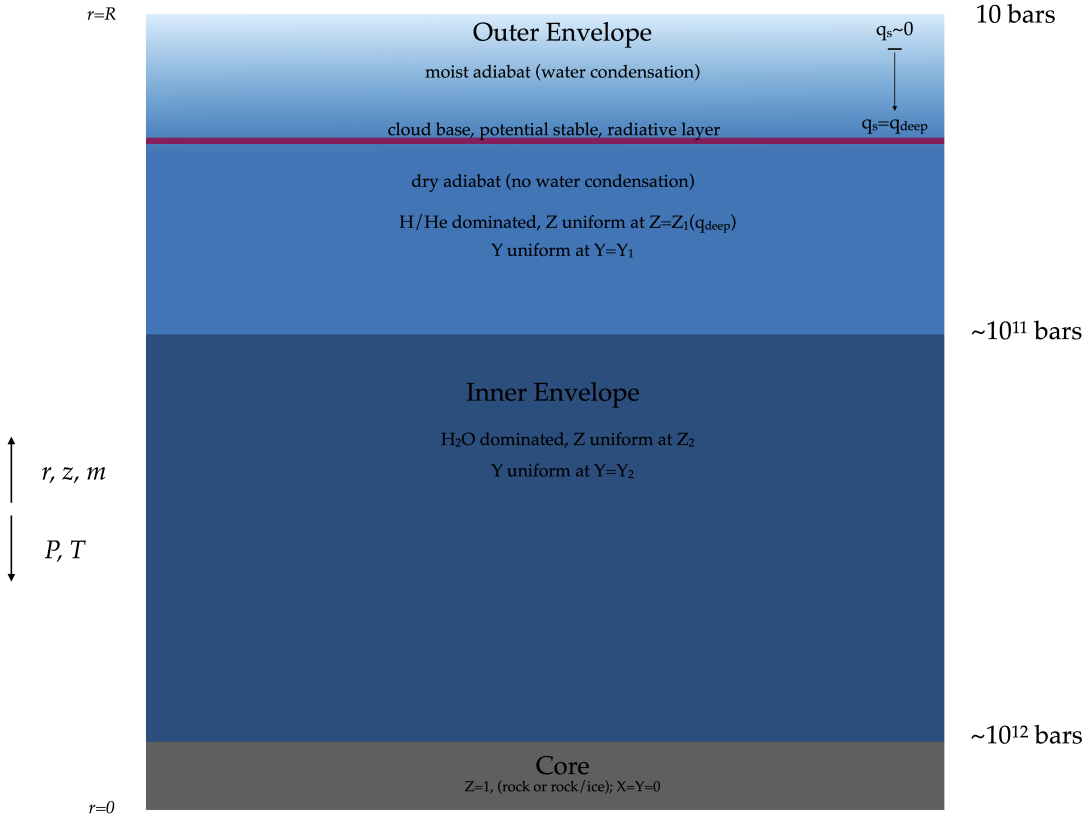


Figure 2.2: The structure for moist adiabatic interior, allowing for condensation-inhibited convection.

inhibited due to the formation of a stable condensation zone when $\alpha < 1$, where α is given by: (Friedson & Gonzales, 2017)

$$\alpha = 1 + \xi(q_s L / R_W T_0) \quad (2.5)$$

If condensation is found to be inhibited,

At pressure where $\alpha < 1$, the cloud base of the water condensation zone forms.

This thin, stable radiative layer has a temperature profile that is governed by:

$$T(P) = T_{\text{top}} + \int_{P_{\text{top}}}^P \left(\frac{dT}{dP} \right)_{\text{rad}} dP \quad (2.6)$$

2.4 Temperature Jump Across the Water Condensation Zone

Letting P_{top} and T_{top} denote the pressure and temperature at the top of the stable water condensation(radiative) zone, the temperature within the radiative zone is given by

$$T(P) = T_{\text{top}} + \int_{P_{\text{top}}}^P \left(\frac{dT}{dP} \right)_{\text{rad}} dP. \quad (2.7)$$

The radiative zone is thin under the relatively opaque conditions typical of water condensation zones in the ice giants (Leconte et al. 2017, Friedson & Gonzales 2017). As a result our discretized model does not spatially resolve the radiative layer. Instead we treat the layer as a discontinuous increase in T and water vapor mole fraction x_{vap} . Here we derive the magnitude of the temperature jump in the limit of a thin radiative zone.

Over a thin layer, the radiative temperature gradient

$$\left(\frac{dT}{dP} \right)_{\text{rad}} = \frac{T}{P} \nabla_{\text{rad}} = \frac{T}{P} \times \frac{3}{16} \frac{\kappa_R P}{g} \frac{T_{\text{int}}^4}{T^4} \quad (2.8)$$

is nearly constant. In this case the integral in (2.7) simplifies to

$$T_{\text{base}} \equiv T(P + \Delta P) = T_{\text{top}} + \left(\frac{dT}{dP} \right)_{\text{rad}} \Delta P. \quad (2.9)$$

Just as in the moist troposphere above, the local water vapor mole fraction x_{vap} follows the saturation value $x_{\text{vap}}^{\text{sat}}$ everywhere within the radiative layer, i.e.,

$$x_{\text{vap}}(P, T) = x_{\text{vap}}^{\text{sat}}(P, T) = \frac{e_s(T)}{P}, \quad P < P_{\text{base}}. \quad (2.10)$$

We denote by P_{base} and T_{base} the pressure and temperature at the base of the radiative zone, which is set by the condition that x_{vap} has reached the deep value $x_{\text{vap}}^{\text{deep}}$:

$$x_{\text{vap}}^{\text{sat}}(P_{\text{base}}, T_{\text{base}}) = \frac{e_s(T_{\text{base}})}{P_{\text{base}}} = x_{\text{vap}}^{\text{deep}} \quad (2.11)$$

$$\implies \Delta P \equiv P_{\text{base}} - P_{\text{top}} = \frac{e_s(T_{\text{base}})}{x_{\text{vap}}^{\text{deep}}} - P_{\text{top}}. \quad (2.12)$$

(Here e_s is the H₂O saturation vapor pressure, calculated from XXXX relation [describe what the method from thermodynamics.py actually does].) Deeper pressures $P > P_{\text{base}}$ are sub-saturated and hence no further condensation of H₂O takes place. ΔP gives the extent, in pressure coordinates, of the radiative layer. Combining (2.12) and (2.7) yields

$$T_{\text{base}} = T_{\text{top}} + \left(\frac{dT}{dP} \right)_{\text{rad}} \left(\frac{e_s(T_{\text{base}})}{x_{\text{vap}}^{\text{deep}}} - P_{\text{top}} \right) \quad (2.13)$$

which we numerically solve for T_{base} . Deeper temperatures are then obtained by integrating the dry adiabat ∇_{ad} :

$$T(P > P_{\text{base}}) = T_{\text{base}} + \int_{P_{\text{base}}}^P \left(\frac{dT}{dP} \right)_{\text{ad}} dP. \quad (2.14)$$

2.5 Thermal Evolution of Model

Conservation of energy relates the instantaneous luminosity profile $L(m)$ to the rate of change of specific entropy s in the planet:

$$\frac{dL}{dm} = -T \frac{\delta s}{\delta t}. \quad (2.15)$$

Integrating over the mass of the planet and solving for δt yields

$$\delta t = -\frac{1}{L_{\text{int}}} \int_0^M T \delta s dm \quad (2.16)$$

where L_{int} is the intrinsic luminosity $4\pi R^2 \sigma_{\text{SB}} T_{\text{int}}^4$.

For our assumed ideal mixture of light elements (H/He) and heavy elements (H₂O) this entropy difference is simply

$$\delta s = (1 - Z)\delta s_{HHe} + Z\delta s_Z \quad (2.17)$$

where in practice δs_Z is computed in terms of the change in internal energy and density:

$$T \delta s_Z = \delta u_Z + P \delta (\rho_Z^{-1}). \quad (2.18)$$

3

Results

3.1 Condensation-inhibited Convection

Talk about Figure 3.1.

3.2 Formation of Radiative Zone

Talk about Figure.

3.3 Thermal Evolution of Uranus and Neptune

Talk about Figure.

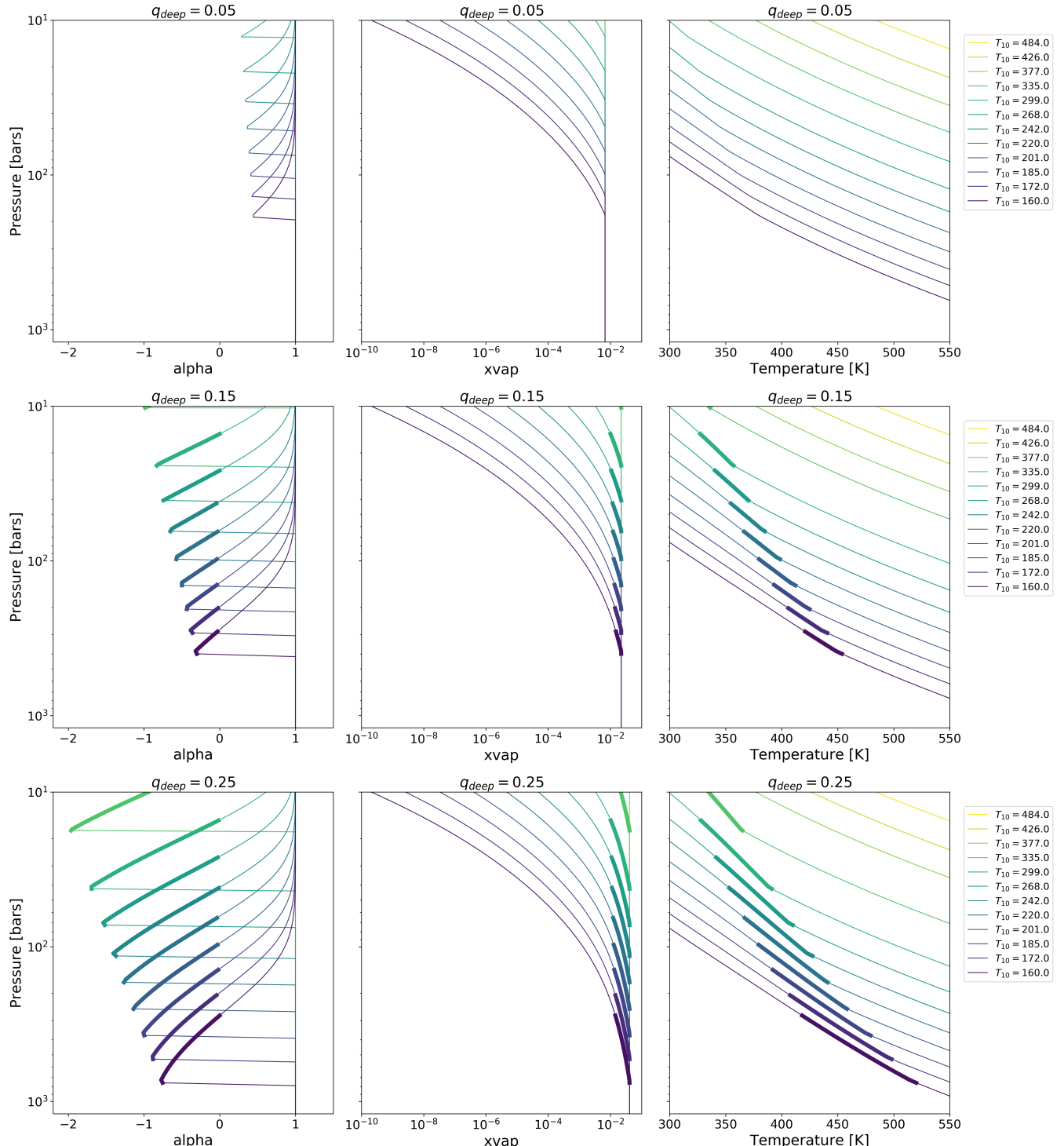


Figure 3.1: add description re: moist adiabat, when/where convection is inhibited and where the radiative zone base is in these plots. explain differences

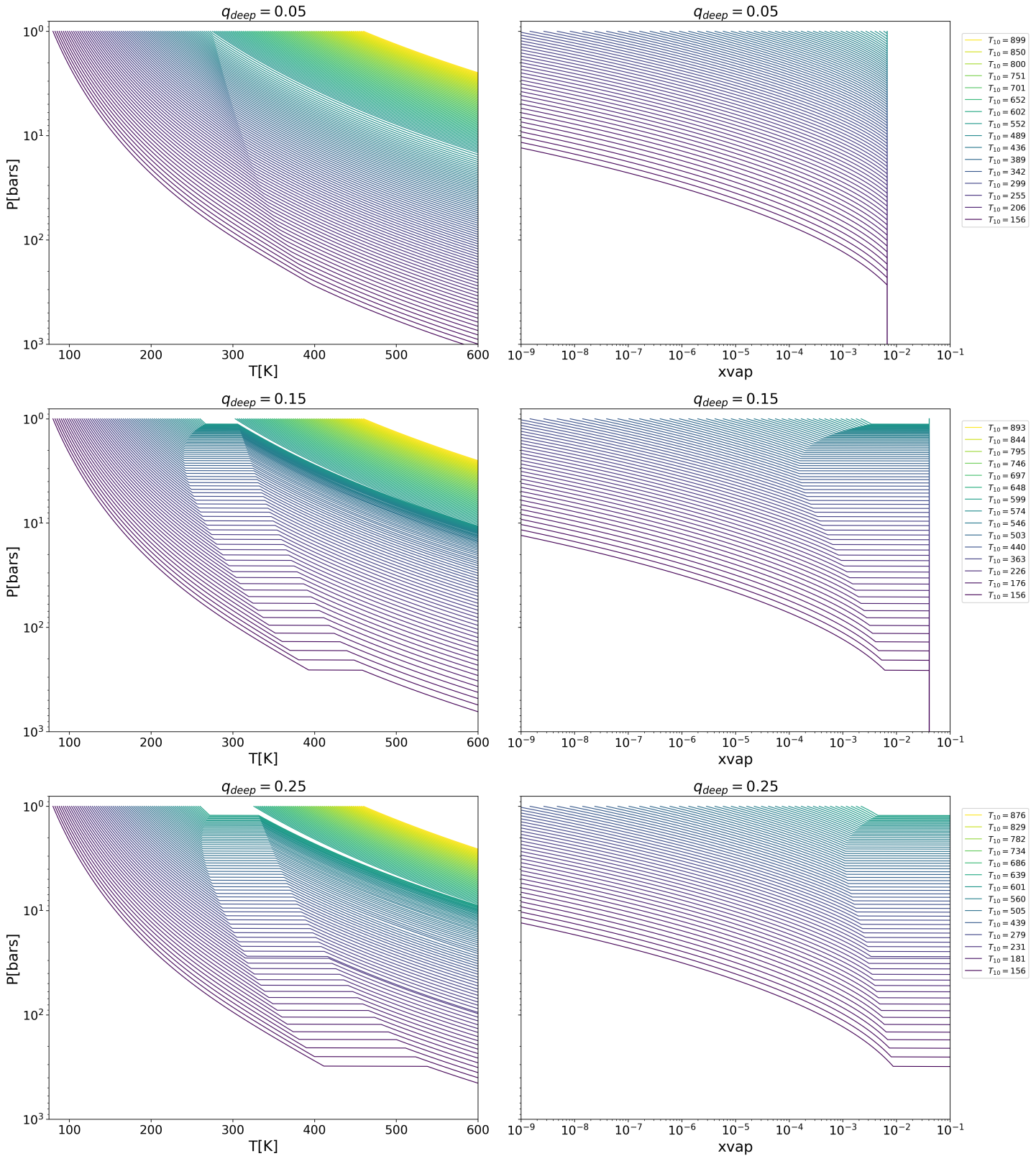
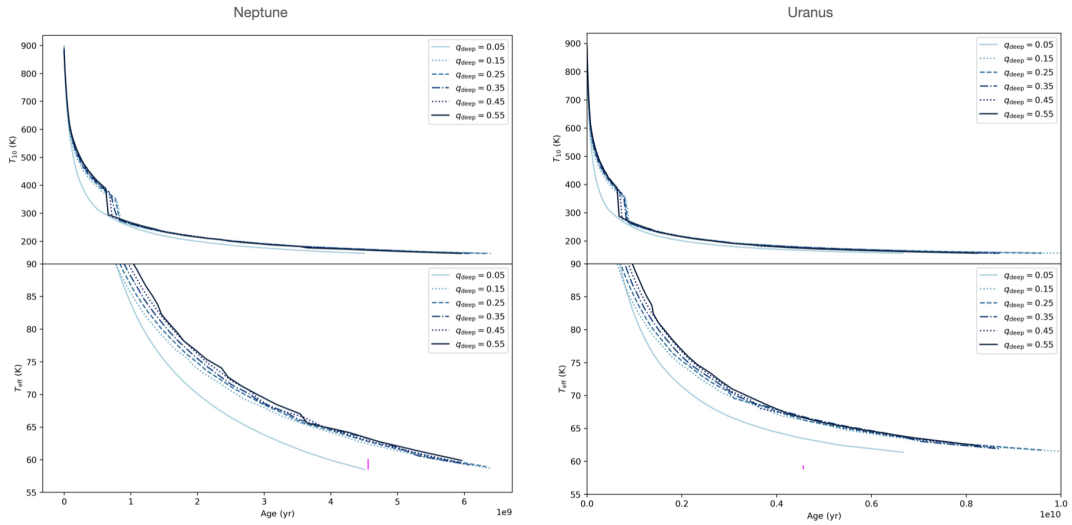
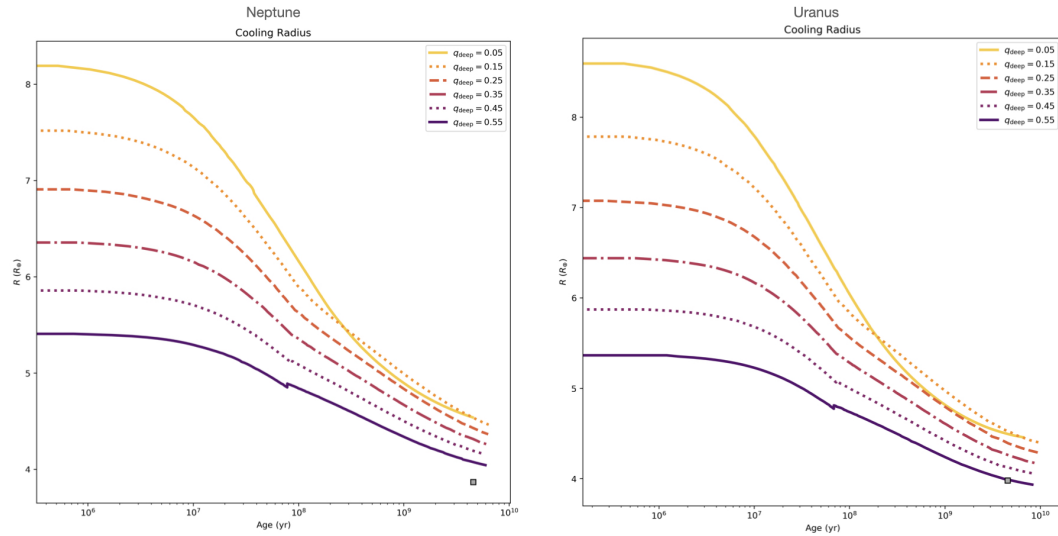


Figure 3.2: add description these plots. explain differences



(a) label 1



(b) label 2

Figure 3.3: 2 Figures side by side

4

Discussion and Conclusions

Appendix A

Some Ancillary Stuff

Bibliography

- Fortney, J. J., Ikoma, M., Nettelmann, N., Guillot, T., & Marley, M. S. (2011). Self-consistent model atmospheres and the cooling of the solar system's giant planets. *The Astrophysical Journal*, 729, 32.
- Friedson, A. J. & Gonzales, E. J. (2017). Inhibition of ordinary and diffusive convection in the water condensation zone of the ice giants and implications for their thermal evolution. *Icarus*, 297, 160–178.
- Guillot, T. (1995). Condensation of methane, ammonia, and water and the inhibition of convection in giant planets. *Science*, (pp. 1697–1699).
- Guillot, T. (2019). Uranus and neptune are key to understand planets with hydrogen atmospheres. *arXiv.org*.
- Harold C. Graboske, Jr., J. B. P. A. S. G. & Olness, R. J. (1975). The structure and evolution of jupiter: The fluid contraction. *The Astrophysical Journal*, 199, 265–281.
- Hubbard, W. (1977a). Comparative thermal evolution of uranus and neptune. *Icarus*, , 35, 177–181.
- Hubbard, W. (1977b). The jovian surface condition and cooling rate. *Icarus*, , 30, 305–310.

- L. Scheibe, N Nettelmann, R. R. (2019). Thermal evolution of uranus and neptune: Adiabatic models. *Astronomy and Astrophysics*, A70, 632.
- Leconte, J., Selsis, F., Hersant, F., & Guillot, T. (2017). Condensation-inhibited convection in hydrogen-rich atmospheres: Stability against double-diffusive processes and thermal profiles for jupiter, saturn, uranus, and neptune. *Astronomy and Astrophysics*, A98, 598.
- Low, F. (1966). Observations of venus, jupiter, and saturn at wavelength 20 microns. *Astronomical Journal*, 71, 391.
- M. Podolak, W.B. Hubbard, D. S. (1991). Models of uranus' interior and magnetic field. *Uranus*, Editors: J.T. Bergstrahl, E.D. Miner, M. Shapely Matthews, (pp.29).
- N. Nettelmann, K. Wangd, J. F. S. H. S. Y. M. B. R. R. (2016). Uranus evolution models with simple thermal boundary layers. *Icarus*, 275, 107–116.
- R. Kippenhahn, A. Weigert, A. W. (2012). *Stellar Structure and Evolution*. Springer.
- S. Mazevet, A. Licari, G. C. & Potekhin, A. Y. (2019). Ab initio based equation of state of dense water for planetary and exoplanetary modeling. *Astronomy & Astrophysics*, A128, 621.
- W.B. Hubbard, D. S. (1995). The interior of neptune. *Neptune and Triton*, Editor: D.P. Kruikshank, (pp. 109).
- Y. Miguel, T. G. & Fayon, L. (2018). Jupiter internal structure: the effect of different equations of state. *Astronomy & Astrophysics*, C2, 618.